Interaction and concerted diffusion of lithium in a (5,5) carbon nanotube

M. Khantha,[1] N. A. Cordero,[1,2] J. A. Alonso,[3] M. Cawkwell,[4] and L. A. Girifalco[1]

[1]*Department of Materials Science and Engineering, University of Pennsylvania, Philadelphia, Pennsylvania 19104, USA*
[2]*Departamento de Física, Universidad de Burgos, E-09001 Burgos, Spain*
[3]*Departamento de Física Teórica, Atómica y Óptica, Universidad de Valladolid, E-47011 Valladolid, Spain*
[4]*Theoretical Division, Los Alamos National Laboratory, Los Alamos, New Mexico 87545, USA*

The interaction and diffusion of lithium atoms in a (5,5) carbon nanotube is studied using density-functional theory. The Li-nanotube interaction perpendicular to the tube axis for a single Li inside and outside the tube is calculated and compared with the Li-graphene interaction obtained using the same technique. Both interactions are similar in the repulsive region but exhibit differences in their attractive part. Nevertheless, they can be described using a common parametrization. The Li-Li interaction is calculated as a function of their separation inside the tube. This interaction is similar to a screened repulsive Coulomb potential at small separations. However, at larger separations, the Li-Li interaction does not vanish and shows residual oscillations. This repulsive long-ranged interaction favors concerted diffusion of many Li atoms compared to the independent diffusion of individual Li inside the tube.

I. INTRODUCTION

The properties of lithium doped carbon nanotubes have been studied extensively over the past decade.[1–11] The early research in this area was initiated by the observation that lithium intercalated carbon nanotubes offered much higher Li capacity (ranging from $Li_{1.6}C_6$ to $Li_{2.7}C_6$ depending on processing conditions[1,4–7]) compared to graphite intercalation compounds (LiC_6 under optimal conditions[8,12–18]). The enhanced Li composition in nanotubes is expected to improve the performance of Li-ion rechargeable batteries.[8,14,18] The doping of single wall carbon nanotube (SWCNT) by Li is also known to increase hydrogen storage capacity.[19,20] Many experimental studies[2,3,6,9,21,22] have been carried out to determine the energetics of lithium adsorption in nanotubes.

Theoretical investigations have focused on the intercalation of Li in SWCNTs,[23–36] in multiwall carbon nanotubes (MWCNTs),[9,21,23,37] and the calculation of energy barriers for entry and diffusion of Li inside the tubes.[24,25,27,29,30,32–34,37–39] The binding energy of Li to nanotubes of different diameters and chiralities has been obtained in several papers[4,23–29,32–35,37,38,40] using *ab initio* methods. The following general features of the Li-tube interaction emerge from these studies: The energies of absorption inside and outside the tube are similar for a single Li atom. Almost complete charge transfer occurs from the Li to the tube walls. The diffusion barrier for the motion of Li inside nanotubes is small, on the order of 100 meV depending on the path, implying fast diffusion. The interaction of Li atoms inside SWCNTs has mostly been inferred[23,24,26–30,38] and calculated explicitly only for a few nanotubes.[26,32] The Li-Li interaction inside the tube is found to be flat and short-ranged with strong screening at small separations. One study[26] noted that weak Li-Li repulsive interactions persisted up to large separations.

Most *ab initio* studies based on density-functional theory[41] (DFT) typically involve different schemes and approximations and consider various types of nanotubes. This makes it difficult to compare the results. A systematic study of how the interaction of Li with the tube walls and with other Li affects the diffusion of Li in the nanotube has not been carried out. The objective of this paper is to analyze in detail the Li-tube and Li-Li interactions for one specific system [a (5,5) carbon nanotube] and understand how it influences the diffusion of Li. Many different configurations of Li atoms in the nanotube are examined. The energies of various configurations can be directly correlated with specific features of both Li-tube and Li-Li interactions that depend sensitively on the position of Li relative to the framework of carbon atoms. The detailed analysis shows that concerted diffusion of many Li ions is more favorable than the uncorrelated motion of individual ions.

The rest of this paper is organized as follows: Section II describes the methodology used and the testing of pseudopotentials. Section III is focused on the Li-tube interaction for a single Li and the parametrization and comparison of this potential with the Li-graphene interaction. Section IV treats the Li-Li interaction inside the nanotube. Section V describes the diffusion of Li inside nanotubes. Section VI presents a summary of the main results.

II. COMPUTATIONAL METHOD AND VALIDATION OF PSEUDOPOTENTIALS

We have used the DFT as implemented in the FHI98MD code[42] in all our calculations. The parametrization by Perdew and Wang[43] was used for exchange and correlation in the local density approximation (LDA). The $(2s^2 2p^2)$ electrons of carbon and the $(2s^1)$ electron of lithium were treated explicitly while the core electrons of C and Li were described by Troullier-Martins pseudopotentials[44] in the Kleinman-Bylander separable form.[45] The Li pseudopotential included an additional nonlinear exchange-correlation interaction between core and valence electrons.[42,46] The electronic wave functions were expanded in a plane-wave basis. The kinetic energy cutoff was set at 680 eV (50 Ry) and all energies were converged to 2.7 meV (10^{-4} Hartree).
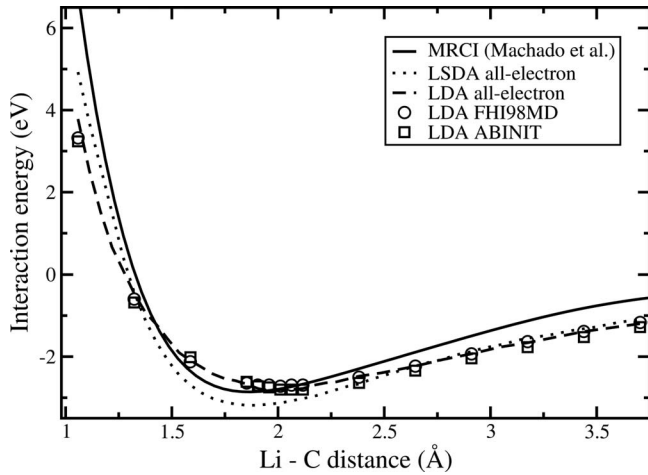
FIG. 1. Interaction energy of the LiC molecule calculated with pseudopotentials using FHI98MD (circles) and ABINIT (squares) codes vs all-electron LDA calculations with (dotted line) and without (dashed line) spin polarization and MRCI results (solid line).

TABLE I. Pseudopotential vs all-electron LDA results for Li-graphene interaction.

Property	Pseudopotential calculations	All-electron calculations
Equilibrium distance (Å)	1.6	1.7
Binding energy at equilibrium distance (eV)	0.93	1.22
Insertion barrier (eV)	7.40	8.08

In our earlier work on the Li-graphene system,[47] the Li and C pseudopotentials were tested individually by calculating bulk properties of graphite and lithium. We now test them together in different Li-C environments. In the first test, we have obtained the interaction energy of the lithium carbide (LiC) molecule using the same pseudopotentials but with two different codes [FHI98MD (Ref. [42]) and ABINIT (Ref. [48])] as well as an all-electron method.[49] The results are presented in Fig. [1]. For comparison, we also show multireference configuration interaction (MRCI) results from Machado *et al.*[50] Isolated points represent the pseudopotential calculations, dotted and dashed curves represent, respectively, all-electron results with (LSDA) and without (LDA) spin polarization and the solid curve corresponds to the MRCI values. The pseudopotentials reproduce all-electron results not only close to the equilibrium configuration but also at small and large Li-C separations. The LSDA result is qualitatively similar to the MRCI result and non-spin-polarized LDA gives a reasonable description of the Li-C interaction.

The second test was done on the Li-graphene system to examine if the pseudopotentials properly describe the sp^2 hybridization of C which occurs in both graphene and nanotubes. We have previously reported[47] the binding energy and equilibrium distance between Li and graphene calculated with the same pseudopotentials. We compare these results with new all-electron LDA calculations for the interaction of a Li with (unrelaxed) graphene using the WIEN2K code[51,52] in Table [I]. The energy barriers for penetration of Li into graphene at the center of a C hexagon are shown in the table for both methods. There is good agreement for the equilibrium distance but the binding energy and energy barrier are smaller for pseudopotential calculations compared to the all-electron values.

Summarizing, the pseudopotentials chosen in this and our earlier work[47] give results in agreement with all-electron calculations for pure phases of Li and C, the LiC molecule, and the Li-graphene system. The pseudopotentials describe Li and C atoms in very different environments and, thus, are

suitable to study interactions in the Li-nanotube system.

A hexagonal supercell with periodic boundary conditions was used to represent the (5,5) nanotube with the *z* direction along the axis of the tube. The length of a hexagonal edge perpendicular to the tube axis was 15.32 Å. A supercell containing 60 carbon atoms (denoted as 60 C with a periodicity of 7.38 Å along *z* axis) was sufficient for calculating the Li-tube interaction perpendicular to the tube axis while a larger supercell containing 120 carbon atoms (denoted as 120 C with a periodicity of 14.76 Å along the *z* axis) was used for Li-Li interactions and diffusion barriers. Configurations with up to 12 Li atoms inside the 120 C supercell were studied while all calculations with the 60 C supercell contained only one Li atom. The Brillouin zone was sampled using the Monkhorst-Pack scheme[53] with two inequivalent *k* points for the 60 C supercell and only the Γ-point for the 120 C supercell.

We define ΔE to be the interaction energy per Li atom given by

$$\Delta E = \frac{1}{n}[E(\text{tube} + n \text{ Li}) - E(\text{tube}) - nE(\text{Li})], \qquad (1)$$

where *n* represents the number of Li atoms per supercell, $E(\text{tube}+n \text{ Li})$ is the energy of the tube with *n* Li atoms, $E(\text{tube})$, the energy of the tube without Li, and, $E(\text{Li})$, the energy of a single Li (all the energies are calculated in the same supercell). The nanotube was relaxed with and without Li. The structural distortion of the tube was very slight and the relaxed total energies differed negligibly from the corresponding values for a rigid tube. Thus, all results are with reference to the unrelaxed tube geometry.

III. LITHIUM-NANOTUBE INTERACTION NORMAL TO THE TUBE AXIS

This section describes the Li-tube interaction perpendicular to the tube axis and its comparison with Li-graphene interaction.[47] The symmetry of the (5,5) tube implies that the most favorable positions for Li are along a straight line passing through the center of a six-member carbon ring on one side of the wall and the midpoint of a C-C bond on the opposite side as shown in Fig. [2]. The intersection of this line with the tube axis is labeled *D*, *B* denotes the center of a carbon ring on the tube wall, and *F* denotes the midpoint of a C-C bond perpendicular to the tube axis. Minima and maxima of the Li-tube interaction occur at special positions along this line and these are shown in the figure. For sim-
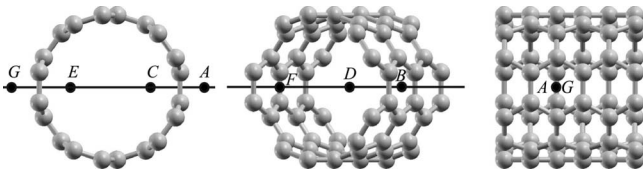
FIG. 2. Axial (left), intermediate (center), and side (right) views of the 60 C supercell as it rotates clockwise (seen from above) around a vertical line perpendicular to the tube axis. The small filled circles represent equilibrium positions (minima shown in left and maxima shown in center) for a Li atom (see Fig. 3). The positions of the maxima and minima coincide in the side view.

plicity, we refer to the carbon ring as a "hexagon" from now on, though it is not contained in a plane.

Figure 3 shows the Li-tube interaction perpendicular to the axis as a function of Li position inside and outside the tube with D taken to be the origin. The origin of the energy axis was taken as the sum of the energies of the pure nanotube and a single Li atom [Eq. (1) with $n=1$]. The curve labeled "LDA 60C cell" in Fig. 3 represents ΔE calculated with the 60 C supercell. Some calculations were done with the 120 C supercell and these results are labeled "LDA 120C cell." The interaction energy in the 60 C supercell is almost the same as in the 120 C supercell. This suggests that the z period of the 60 C supercell is sufficient to study the interaction along a line perpendicular to the axis. ΔE is nearly zero when the Li is close to the sidewall of the supercell (7.66 Å). This implies that the supercell dimension perpendicular to the axis (15.32 Å) is sufficient to avoid the interaction between the Li atom and the carbon nanotube from an adjacent supercell. To check the validity of the results based on LDA, Fig. 3 also shows the interaction energy calculated using the Becke-Lee-Yang-Parr (BLYP) (Refs. 54 and 55) generalized gradient approximation (GGA) for the exchange-correlation functional. As seen from the plot, there is no significant difference between using LDA and GGA in accordance with recent results.[40]

Starting from the right in Fig. 3, position A represents an energy minimum when Li is bound outside the tube; B, a

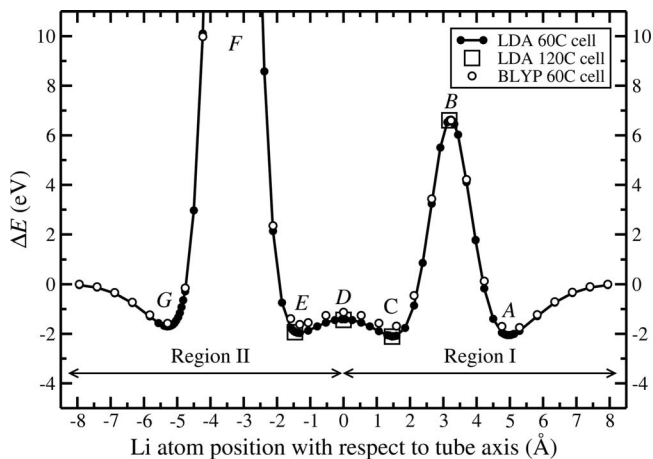
FIG. 3. The Li-tube interaction along a line perpendicular to the tube axis and passing though the center of a carbon hexagon (see Fig. 2). The labels are explained in the text and the corresponding energies are listed in Table II.

TABLE II. Equilibrium positions of Li and their energies perpendicular to the tube axis (see Figs. 2 and 3).

Position of Li atom	Distance to tube axis (Å)	ΔE (eV)
Minimum A	4.97	−2.05
Maximum B	3.22	6.64
Minimum C	1.46	−2.11
Maximum D	0.00	−1.41
Minimum E	1.31	−1.97
Maximum F	3.32	
Minimum G	5.29	−1.70

maximum when the Li is at the center of a hexagon on the tube wall; C, a minimum when Li is bound inside the tube in Region I; D, a maximum when Li is on the axis of the tube; E, a minimum when Li is bound inside in Region II; F, a maximum (not calculated because structural relaxation is important in this case) when Li is at the midpoint of a C-C bond, and, G, a minimum when Li is outside the tube. The positions of the extrema and their corresponding energies (calculated with LDA) are given in Table II.

Position C inside the tube is marginally more favorable for binding Li than position A on the outside (the difference in energy is 0.06 eV). The results for position C are in good agreement with earlier calculations: Meunier *et al.*[27] obtained an equilibrium distance of 1.29 Å using LDA and Zhao *et al.*[34] obtained 1.33 Å using GGA with interaction energy equal to −2.33 eV (occasionally, both LDA and GGA calculations[40] give an opposite result where Li binds more strongly to the outside than to the inside of the tube). Comparing the two minima inside the tube, Li is bound more strongly to the tube at position C than at E in conformity with earlier results. The energy barrier for inserting a Li atom through the (unrelaxed) tube wall is the interaction energy at B, namely, 6.64 eV [smaller than the barrier in the case of the graphene sheet (see Table I) due to the curvature]. The static diffusion barrier for the entry of Li from outside the tube is the difference in interaction energy between minimum A and maximum B, equal to 8.75 eV from Table II. This value is numerically smaller than the ones obtained earlier by Meunier *et al.*[27] using LDA (13.5 eV) and Nishidate and Hasegawa[40] using both LDA (9.70 eV) and GGA (10.12 eV). Nevertheless, Li diffusion through the tube wall for temperatures below the melting point of the tube is impossible even for this smaller value.

The Li-tube interaction shown in Fig. 3 and the Li-graphene interaction obtained earlier[47] can be compared effectively if both potentials are plotted using a common reference wall. The graphene sheet defines the "wall" for the Li-graphene interaction as it corresponds to an energy maximum. The "geometric" tube wall is a cylindrical surface of radius $r=3.39$ Å for the unrelaxed tube. The energy maxima B and F are not on the geometric wall: B is located at $r'=3.22$ Å in Region I while F is located at $r''=3.32$ Å in Region II. The difference between the locations of the "geometric" and "energy" walls is due to the curvature of the
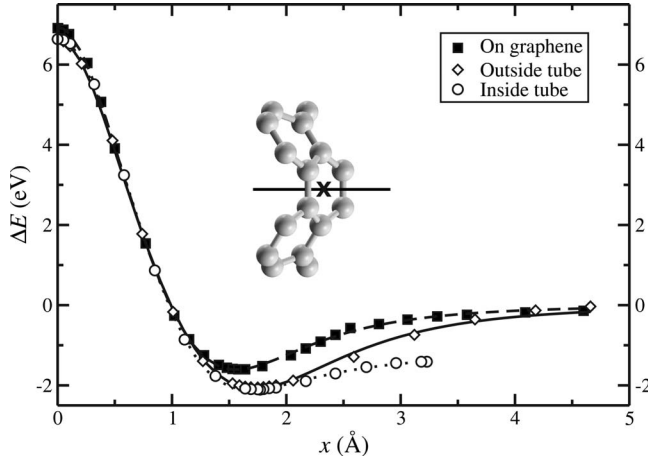
FIG. 4. Lithium interaction with graphene and nanotube vs distance to the wall. The Li is located on top of the center of a carbon hexagon. The squares represent the interaction with graphene, diamonds, with the tube from outside and circles, with the tube from inside. The lines represent fitted potentials (see text for details).
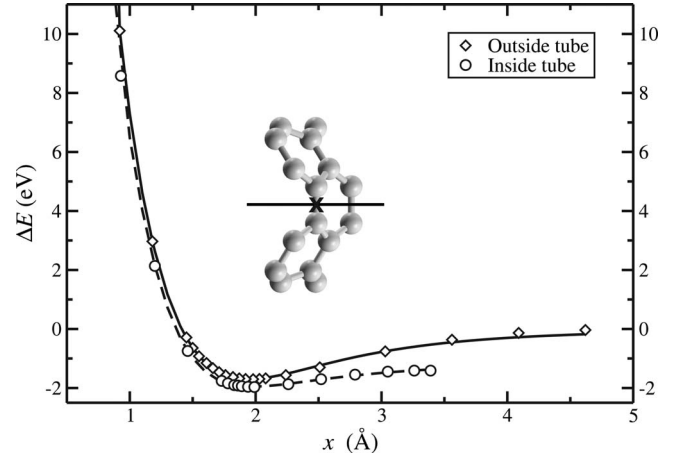

FIG. 5. Lithium interaction with nanotube vs distance to the wall. The Li is located on top of the center of a C-C bond. The diamonds represent the interaction from the outside and circles, the interaction from the inside. The lines represent fitted potentials (see text for details).

tube. Consider the Li atom at B. It has six first-neighbor C atoms that form a bent hexagon. If this hexagon was planar (as in graphene) the maximum repulsion would be located at the center of the hexagon and the geometric and energy wall would coincide. The curvature of the tube moves maximum B inward to $r' = 3.22$ Å. At position F, Li has only two first-neighbor C atoms forming a C-C bond on the tube wall. Elemental geometry shows that the midpoint of this bond is at $r'' = 3.32$ Å.

Figure 4 shows the Li-tube interaction when Li is positioned in Region I and the Li-graphene interaction calculated earlier.[47] Both potentials are plotted versus the distance to the "energy wall" (denoted by x). The interaction energies inside and outside the tube are virtually identical from close to the energy wall up to the equilibrium positions which are 0.03 Å apart: There are differences in the attractive part because the potential outside the tube tends to zero while inside the tube the interaction reaches a maximum on the tube axis ($x = r'$). [For $r > r'$, Li is attracted to minimum E (Fig. 3) and this is shown in Fig. 5.] There are also differences at very small distances and at the equilibrium position because the lithium atom sees a planar carbon hexagon in the case of graphene and a nonplanar hexagon in the case of the tube. Figure 5 shows the Li-tube interaction perpendicular to the axis for Li inside and outside the tube in Region II using the

energy wall r'' as the origin. The repulsive interaction inside and outside the tube is almost identical but the agreement is not so close (the two minima are 0.04 Å apart and the difference in energy is 0.27 eV) as in Region I (Fig. 4). Once again, the differences are bigger in the attractive part due to boundary conditions.

A common parametrization that represents both Li-graphene and Li-tube interactions normal to the lattice is useful because it can serve as an empirical potential in large-scale simulations. The Li-nanotube and Li-graphene potentials in both Regions I and II (plotted with the energy wall as the reference) can be fitted using the following simple analytical form:

$$U(x) = \frac{a_1 + a_2 x^2 + a_3 x^6}{a_4 + a_5 x^2 + a_6 x^6}, \qquad (2)$$

where x represents the distance to the energy wall. This (0–2–6)/(0–2–6) Padé rational function is flexible enough to suit Li-tube and Li-graphene interactions both at short and long distances. The fitting parameters are presented in Table III and the fitted potentials are shown in Figs. 4 and 5 as curves. The parametrization reproduces the calculated results for all cases. The differences in the values of fitting parameters for Li-nanotube and Li-graphene interactions are largely a con-

TABLE III. Li-nanotube and Li-graphene potential parameters. [See Eq. (2) for details.]

Position of the atom	a_1 (eV)	a_2 (eV/Å^2)	a_3 (eV/Å^6)	a_4	a_5 (1/Å^2)	a_6 (1/Å^6)
Li inside the nanotube in Region I	−63.2034	64.4777	2.4385	−9.46424	−9.65027	−2.02597
Li outside the nanotube in Region I	2077.96	−2117.47	0	313.188	356.450	24.9606
Li on graphene on top of the center of a carbon ring	1750.25	−1808.07	0	252.492	301.222	46.0551
Li inside the nanotube in Region II	188.55	−92.9801	−2.2245	2.96523	9.47502	1.96947
Li outside the nanotube in Region II	−43800.6	21944.2	0	−102.803	−2656.77	−238.355

sequence of the form of the Padé function. Taylor expansions of the fitted potentials at short (close to the carbon wall), intermediate (around the equilibrium position), and long (far from the wall) distances show that the interactions are quite similar (as can be seen in Figs. 4 and 5). In our earlier work,[47] we had fitted the Li-graphene potential as a sum of two functions: a screened Coulomb interaction resulting from the charge transfer between Li and C atoms and a modified Lennard-Jones interaction with an asymptotic decay of x^{-4}. The form chosen in Eq. (2) has the same asymptotic decay when the coefficient $a_3=0$. As seen from Table III, the Li-graphene and the Li-tube interactions for Li outside the tube have been fitted with $a_3=0$ to match the asymptotic decay to the earlier work. The well-known difficulties of the LDA to reproduce long-range van der Waals interactions have been discussed in our earlier work.[47] However, because of the sizable charge transfer, the main contribution to the interactions in the Li-nanotube and Li-graphene systems is of electrostatic origin, and the van der Waals contribution is minor at the relevant distances. Therefore, the calculations presented above are expected to be correct not only in the repulsive region and near the equilibrium distance, but also for separations substantially larger than the equilibrium distance, as noted before.[47]

Thus, the versatile Padé form enables us to fit both the screened Coulomb interaction at small separations and the different forms of asymptotic behavior for Li inside and outside the nanotube. The existence of a simple analytical form that describes the adsorbate-lattice interaction from the lattice wall to large distances lends support that a universal potential as found for pure graphitic-carbon systems[56] may also exist when Li ions are also present in such structures.

IV. LITHIUM-LITHIUM INTERACTION INSIDE THE NANOTUBE

In this section, we examine how two or more Li atoms interact inside the nanotube. All calculations have been done using the 120 C supercell. The relaxation of two Li atoms showed that both Li were aligned parallel to the axis at the same distance as found for a single Li atom (1.46 Å) and the lowest energy Li-Li separation was 7.38 Å (the maximum value allowed in this supercell). We consider a linear chain positioned at 1.46 Å from the tube axis with two, three, four, or six Li atoms in the supercell to study the Li-Li interaction inside the tube. This simple arrangement enables a systematic evaluation of Li-Li interactions with separation. The periodicity of the supercell along the tube axis implies that an infinite chain of Li atoms is positioned parallel to the tube axis inside adjacent 120 C supercells. The charge-charge interaction between Li in neighboring supercells perpendicular to the tube axis is negligible due to the effective screening by tube walls and due to the large lateral size of the supercell. Figure 6 shows a sample of the different arrangements examined. Configuration a serves as a reference and contains only one Li atom per supercell. The linear chain contains two Li atoms per supercell in configurations b, f-i and three Li atoms per supercell in configurations c and j. Configurations d and e contain, respectively, a linear chain with four and six
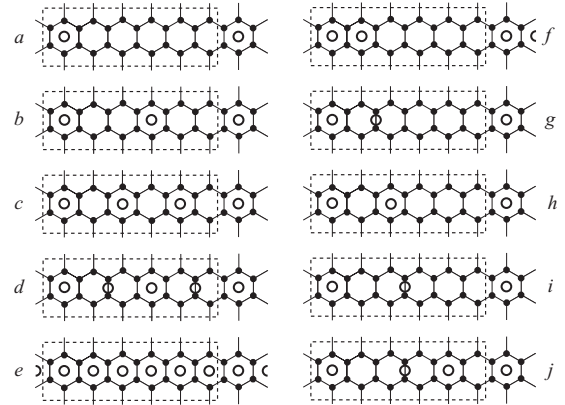

FIG. 6. A selection of configurations used to study Li-Li interactions inside the (5,5) tube. Only the carbon atoms (solid circles) close to the chain of Li atoms (empty circles) are shown for clarity. The solid lines represent C-C bonds and the dashed line shows the size of the 120 C supercell along the tube axis. The Li atoms are evenly spaced in the left column and unevenly spaced in the right column.

atoms per supercell. Table IV lists ΔE, the interaction energy per Li atom, for all the configurations shown in Fig. 6.

Figure 7 shows the interaction energy per Li atom, as a function of the Li-Li separation when only two Li atoms are inside the supercell. The energy of configuration a in Fig. 6 (with only one Li in the supercell) was taken as energy origin. We also include for comparison the interaction energy per Li in a Li dimer (lower curve in Fig. 7) calculated under the same conditions but without the nanotube (in both cases the results for separations below 1.7 Å are only qualitative because the core radius[47] of the Li pseudopotential used is 0.84 Å). The dimer interaction has a minimum located at 2.71 Å in good agreement with earlier LDA all-electron calculations (2.72 Å) (Ref. 57) and close to the experimental binding distance (2.67 Å).[58]

The repulsion between Li ions inside the tube is greater than the repulsion between neutral Li atoms forming the dimer. Nevertheless there is screening of the Li-Li repulsion inside the tube and the interaction can be fitted to a screened

TABLE IV. Interaction energy and diffusion barrier per Li atom for configurations shown in Fig. 6.

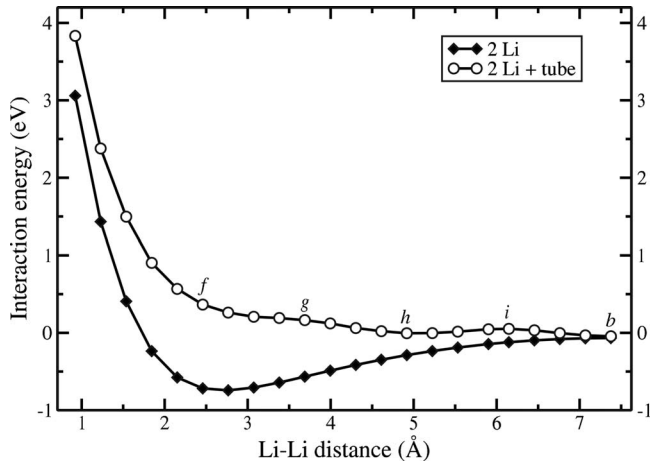| Number of Li atoms in the supercell	Configuration	Interaction energy per Li (eV)	Barrier (meV)
1	a	−2.112	177
2	b	−2.157	175
3	c	−2.126	175
4	d	−1.924	11
6	e	−1.425	128
2	f	−1.747	174
2	g	−1.949	9
2	h	−2.117	180
2	i	−2.060	6
3	j	−2.033	42

FIG. 7. Interaction energy per Li atom as a function of Li-Li separation for a two-atom chain. The interaction energy per Li for a Li dimer without the tube is given for comparison. See Fig. 6 for the geometry of the labeled configurations.

Coulomb potential at small separations (<2 Å). At larger separations (>3.7 Å), the interaction clearly displays an oscillatory character that extends up to the maximum separation of 7.38 Å. This feature arises from two separate effects: (i) The Li-Li repulsion is a monotonically decreasing interaction that extends to large separations between the ions due to incomplete screening; (ii) The Li-tube interaction also contributes to ΔE and its magnitude depends on the position of Li with reference to the hexagonal carbon framework. As seen from Table II, Li located on top of centers of hexagons (minimum C) have lower energy compared to Li located on top of the midpoint of a C-C bond (minimum E). Both positions represent equilibrium inside the tube but with a small difference in energy on the order of 0.1 eV. The Li-tube contribution is thus modulated as a function of Li-Li separation. Special configurations where both Li atoms are located on top of centers of hexagons are *more* favored energetically than separations where one Li is on top of the midpoint of C-C bond. This "fine" feature leads to an oscillation of ΔE parallel to the tube axis. Since the contribution from the modulation is small, the oscillatory feature of the Li-Li interaction (ΔE) is observed only at large separations (>3.7 Å) when its magnitude is not negligible compared to that from ion-ion repulsion.

In principle, the special separations giving rise to a local minimum in ΔE can correspond to any integer multiple of 2.46 Å (the distance between the centers of neighboring hexagons). Configurations *b* and *h* (Fig. 6) with Li-Li separation of 7.38 Å and 4.92 Å, respectively, correspond to local minima in Fig. 7. Configuration *f* where the Li-Li separation is only 2.46 Å is not a local minimum because the ion-ion repulsion is large (>0.1 eV) and effectively masks the small "geometric" modulation. Configurations *g* and *i* are local maxima and correspond to one Li located on top of the center of a hexagon and the other on top of the midpoint of a C-C bond.

Configurations *c*, *d*, and *e* represent, respectively, three, four, and six equidistant Li atom chains in the supercell while configuration *j* corresponds to a three-atom chain with unequal separations. As the number of Li atoms increases, ΔE exhibits additional local minima and maxima due to more possibilities of placing Li atoms on top of centers of hexagons and C-C bonds. The long-range oscillatory character of the Li-Li interaction persists for higher Li densities. Earlier calculations[23,26,27,34] on (5,5) and other nanotubes have noted that the Li-Li interaction inside the tube is long ranged. However, many of these calculations predict a rather flat Li-Li potential for separations larger than 3 Å. Our results show many metastable positions of Li atoms with similar interaction energies per Li. Comparing the energies of configurations *a* and *b* in Table IV suggests that the oscillatory character of Li-Li interactions may also persist for separations larger than 8 Å (a range which can be probed only by going to supercells larger than 120 C). The significance of such long-range oscillations and their effect on the diffusion of Li is discussed in Sec. V.

V. DIFFUSION OF LITHIUM INSIDE THE (5,5) NANOTUBE

The diffusion of Li inside nanotubes has been studied extensively.[24,25,27,29,30,32–34,37–39] The independent diffusion of individual Li atoms has been considered by a combination of *ab initio* and simulation methods. The energy barriers have been calculated over either fixed paths ("constrained" diffusion) or "unconstrained" paths where the movement of Li inside the tube is not restricted. The following results are specific to (5,5) nanotubes: The diffusion barrier for individual Li atoms is very low[24,25,27,29,30,32–34,37–39] implying fast diffusion. Recent studies[32–34] have found that a helicoidal path has a lower barrier than a path parallel to the tube axis. Dynamical simulations[27] have shown Li ions arranged over a cylindrical surface of radius 2.1 Å inside the tube. Our objective is to examine how the diffusion mechanism is affected by the long-ranged oscillatory Li-Li interaction.

Concerted diffusion of chains or clusters of atoms has been proposed for surface adsorbates,[59–64] molecules inside sieves[65–67] and for Li, Na, and K ions inside biological ion channels.[68–70] This process often occurs when there is a mismatch between the equilibrium positions (minima) of the adsorbate-lattice interaction and the adsorbate-adsorbate interaction.[65,66] In situations where the adsorbate-adsorbate interaction is mainly repulsive, concerted diffusion can become viable if there are many metastable positions of the adsorbates with almost similar energies. This is the case for ions diffusing inside ion channels[68] where the metastable positions are located at special values related to the structure of the channel. The potential energy landscape as a function of ion-ion separation is then relatively flat on a coarse scale but exhibits small humps and valleys on a "fine" scale. This feature promotes the concerted movement with a very low energy barrier because contributions from adjacent adsorbates nearly cancel as the humps and valleys of the energy landscape are sampled by many adsorbates concurrently.

The Li-Li interaction discussed in Sec. IV exhibits many of the features that are known to favor concerted diffusion. We now examine if this process is more favorable for diffusion of Li inside the (5,5) nanotube. We obtain the diffusion
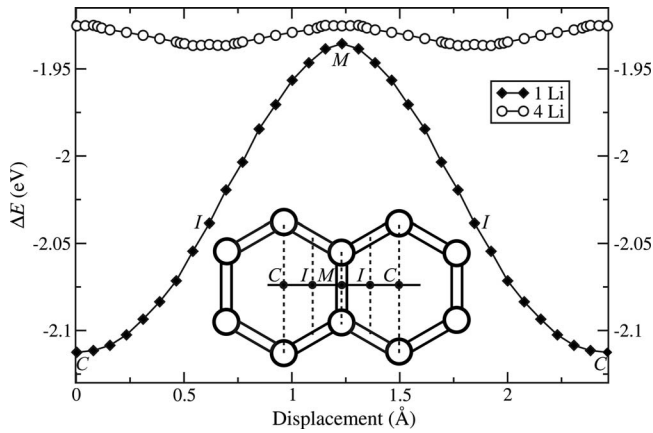
FIG. 8. Interaction energy per Li atom of evenly spaced lithium atoms inside a (5,5) carbon nanotube as a function of the displacement along the tube axis. The two curves correspond to 1 Li and 4 Li chains in the 120 C supercell. Zero displacement refers to configuration a for 1 Li and configuration d for 4 Li (see Fig. 6). The inset is a schematic of special Li positions (filled circles) with respect to the carbon network (open circles). See text for explanation of labels.

barrier for individual Li atoms and compare it with the barrier for the concerted movement of several Li atoms. All barriers are calculated using the 120 C supercell. In both cases, we consider a "constrained" pathway that always maintains the Li atoms at the equilibrium distance perpendicular to the tube axis (i.e., the Li lie on a line parallel to the tube axis at a distance of 1.46 Å and only undergo displacements along this line).

The static diffusion barrier is obtained as follows: Starting with a given configuration, we calculate ΔE as a function of Li displacement (the same for all atoms) along the constrained path. The diffusion barrier is the difference between the maximum and minimum energy configurations along this path. When the supercell contains a single Li atom, the barrier corresponds to nearly independent diffusion because the Li-Li interaction from adjacent supercells is negligible. When the supercell contains two or more Li atoms, the barrier refers to concerted diffusion. It is convenient to use labels C, M, and I (see inset of Fig. 8) to represent Li positions at the top of center of a hexagon, the midpoint of a C-C bond, and the midpoint between C and M, respectively.

The lower curve in Fig. 8 shows ΔE for a single Li as a function of its displacement along the constrained path. It is a symmetric curve with a maximum at M and two equivalent minima at C separated by 2.46 Å. The "constrained" diffusion barrier is 177 meV for a single Li. The upper curve in Fig. 8 shows ΔE as a function of Li displacement for a chain of four equidistant Li atoms in the supercell. The configuration at the origin corresponds to the arrangement $CMCM$ (d in Fig. 6) and is a local maximum in the interaction energy as explained in Sec. IV. An equivalent configuration with the same energy as d is reached when all four Li atoms are displaced rigidly by 1.23 Å, the periodicity of ΔE for the upper curve. The arrangement $IIII$ (that is, with the four Li atoms at I positions) corresponds to the local minimum energy configuration for a chain of four equidistant Li atoms

separated by 3.69 Å. The constrained barrier per Li for the concerted diffusion of the chain is just 11 meV compared to 177 meV for a single Li. There is a very low energy barrier between configurations $IIII$ and $CMCM$ because half the Li atoms are displaced downhill (from I to C) while the remaining half are displaced uphill (from I to M) making the net activation energy very small. The calculated maximum and minimum energy configurations of the four-atom chain are very slightly shifted from the geometric positions labeled as $CMCM$ or $IIII$ above. However, the diffusion barrier changes by less than 1 meV by this offset.

The static diffusion barrier for a linear chain of one, two, three, four, or six Li atoms in the supercell (see Fig. 6 for specific configurations) is listed in the last column of Table IV. The barrier for concerted diffusion varies with the Li density and Li-Li separation. If the Li-Li separation is an integer multiple of 2.46 Å as in configurations b, c, f and h, the local minimum and maximum energy configurations correspond to the arrangements $CCC…$ and $MMM…$, respectively. The activation barrier for concerted diffusion is almost the same as the barrier for single atom diffusion (177 meV), because all Li are displaced uphill from C to M positions as in the case of a single Li. The very small differences in the barrier for configurations b, c, f and h are due to the small changes in the amplitude of the oscillating Li-Li interaction at different separations. Configuration e corresponds to a Li-Li separation of 2.46 Å in the arrangement $CCC…$ with one Li for every carbon hexagon along the supercell. At this separation, the screened ion-ion repulsion is much bigger than the modulations due to the Li-tube interaction. The diffusion barrier for e is considerably lower than the barrier for a single Li because the energies of arrangements $CCC…$ or $MMM…$ are not expected to vary as much as for corresponding arrangements in b, c, f and h where both ion-ion repulsion and Li-tube interaction contribute appreciably to ΔE.

The arrangement of Li in configurations g and i are of the type $CMCM…$. Thus, as explained for configuration d in Fig. 8, the concerted barrier is expected to be similar to that of d and this is indeed observed. Once again, the small differences between the barriers for d, g, and i are related to changes in the amplitude modulation of the Li-Li interaction for large separations. Configuration j has an odd number of Li atoms in the supercell with the arrangement $CMCCMC…$ with unequal separations between the Li. The concerted diffusion barrier is higher than those obtained for even number of Li atoms due to uneven cancellations in the total activation energy. Summarizing all the results shown in Table IV, the trends suggest several configurations for which concerted diffusion along constrained paths has lower activation energy than that of a single atom.

We have calculated the Li-tube interaction for a single Li placed on radial lines different from the one considered earlier (Fig. 2). In all cases, the variation of ΔE is similar to that found in Sec. III. Positions of Li which are closer to C (Fig. 8) have lower energy than positions closer to M. We have also calculated the static diffusion barrier of a single Li for two additional pathways different from that shown in Fig. 8. Consider an unconstrained planar path where the distance of Li to the tube axis is not fixed at the equilibrium value of

1.46 Å. The atom can then be displaced away from the tube wall when its path approaches the midpoint of a C-C bond. The barrier in this case is just the difference between the energies corresponding to Li positions C and E in Fig. 3. Using Table II, the unconstrained barrier is 142 meV. This is smaller than the constrained barrier for a single Li (177 meV) but larger than those previously reported [35 meV (Ref. 27) and 79 meV (Ref. 34)] for unconstrained planar motion of single Li atoms. This discrepancy could be due to differences in the methods used: In our calculations the barrier is obtained as the difference in energies between two static equilibrium configurations. In the earlier papers, the barrier was estimated by dynamical methods where a Li ion samples the energy landscape by moving under the influence of a constant force.

We have also calculated the diffusion barrier for a helicoidal but constrained path such that the distance of the Li from the tube axis remains fixed at 1.46 Å. We obtained a barrier of 94 meV which is again larger than earlier results [46 meV (Ref. 34)] possibly for the same reason. Nonetheless, the barrier for the helicoidal path is smaller than the constrained and unconstrained barriers (177 meV and 142 meV, respectively) calculated for planar paths. This trend is in conformity with the finding[34] that a helicoidal path leads to the minimum barrier for a single Li diffusion along the tube.

In addition to the linear chain discussed in Sec. IV, we have also considered other arrangements where the number of Li atoms in a 120 C supercell ranges between 2 and 12. In some of these, Li atoms are positioned in a zigzag manner on opposite sides of the tube axis at different locations (C, M, I, etc.) and separations inside the tube. ΔE, the binding energy per Li, displays the same trends as those found in Sec. IV: There are numerous metastable positions of Li inside the tube with ΔE varying in a narrow range (-1.90 to -2.16 eV). For example, six Li atoms arranged in a zigzag manner have nearly the same ΔE (in the range -1.90 to -1.92 eV depending on Li positions) as a linear chain of 4 Li discussed in Sec. IV. A distribution of 12 Li atoms on a plane containing the tube axis has a lower ΔE (-1.53 eV) than a linear chain of six Li atoms (-1.43 eV). In general, for similar positions of Li, ΔE is lower for a configuration with larger Li-Li separation than with a smaller separation. The analysis of many such configurations shows that the Li-Li interaction displays oscillations along directions other than those considered in Sec. V. The energy landscape of Li inside the tube thus consists of many small barriers separating metastable states of similar energies superposed on a monotonically decaying repulsive interaction. This energy profile suggests that concerted diffusion of many Li will be favored even along helicoidal and other unconstrained paths.

VI. SUMMARY

We have discussed two aspects of Li interactions inside the (5,5) nanotube: (i) the interaction of a single Li atom with the tube along a line perpendicular to the tube axis and (ii) the Li-Li interaction along the tube axis. The two interactions have the following features: The binding of Li at position C is stronger than at position M (see inset of Fig. 8) but the difference in energies is small. A common parametrization describes the Li-tube and Li-graphene interactions for all positions of Li. The Li-Li interaction inside the tube is long-ranged (persists up to 8 Å or more). At small separations between Li, the interaction is similar to a screened Coulomb repulsion. At long ranges, the interaction displays oscillations due to incomplete screening of ion-ion repulsion superposed with the modulation of Li-tube interaction along the axis. This oscillatory ion-ion repulsion then favors the concerted diffusion of many Li atoms compared to the independent diffusion of individual atoms. The barrier for concerted diffusion depends on the density and geometric arrangement of Li atoms. It is an order of magnitude smaller than that for individual Li inside a (5,5) nanotube.

ACKNOWLEDGMENTS

[1] V. A. Nalimova, D. E. Sklovsky, G. N. Bondarenko, H. Alvergnat-Gaucher, S. Bonnamy, and F. Beguin, Synth. Met. **88**, 89 (1997).

[2] A. Claye and J. E. Fischer, Mol. Cryst. Liq. Cryst. Sci. Technol., Sect. A **340**, 743 (2000).

[3] A. S. Claye, J. E. Fischer, C. B. Huffman, A. G. Rinzler, and R. E. Smalley, J. Electrochem. Soc. **147**, 2845 (2000).

[4] B. Gao, A. Kleinhammes, X. P. Tang, C. Bower, L. Fleming, Y. Wu, and O. Zhou, Chem. Phys. Lett. **307**, 153 (1999).

[5] B. Gao, C. Bower, J. D. Lorentzen, L. Fleming, A. Kleinhammes, X. P. Tang, L. E. McNeil, Y. Wu, and O. Zhou, Chem. Phys. Lett. **327**, 69 (2000).

[6] H. Shimoda, B. Gao, X. P. Tang, A. Kleinhammes, L. Fleming, Y. Wu, and O. Zhou, Phys. Rev. Lett. **88**, 015502 (2001).

[7] H. Shimoda, B. Gao, X. P. Tang, A. Kleinhammes, L. Fleming, Y. Wu, and O. Zhou, Physica B (Amsterdam) **323**, 133 (2002).

[8] M. Monthioux, Carbon **40**, 1809 (2002).

[9] L. Duclaux, Carbon **40**, 1751 (2002).

[10] R. Larciprete, L. Petaccia, S. Lizzit, and A. Goldoni, Phys. Rev. B **71**, 115435 (2005).

[11] V. Lemos, S. Guerini, S. M. Lala, L. A. Montoro, and J. M. Rosolen, Microelectron. J. **36**, 1020 (2005).

[12] R. Juza and V. Wehle, Naturwiss. **52**, 560 (1965).

[13] D. Guerard and A. Herold, Carbon **13**, 337 (1975).

[14] M. S. Dresselhaus and G. Dresselhaus, Adv. Phys. **30**, 139 (1981).

[15] G. Pistolia, *Lithium Batteries: New Materials, Developments, and Perspectives* (Elsevier, New York, 1994).

[16] J. R. Dahn, T. Zheng, Y. Liu, and J. S. Xue, Science **270**, 590 (1995).

[17] J. E. Fischer, Chem. Innovation **30**, 21 (2000).

[18] P. M. Ajayan and O. Z. Zhou, in *Topics in Applied Physics*, edited by M. S. Dresselhaus, G. Dresselhaus, and P. Avouris (Springer-Verlag, Heidelberg, 2001), Vol. 80, p. 391.

[19] P. Chen, X. Wu, J. Lin, and K. L. Tan, Science **285**, 91 (1999).

[20] I. Cabria, M. J. Lopez, and J. A. Alonso, J. Chem. Phys. **123**, 204721 (2005).

[21] G. Maurin, C. Bousquet, F. Henn, P. Bernier, R. Almairac, and B. Simon, Chem. Phys. Lett. **312**, 14 (1999).

[22] R. S. Lee, H. J. Kim, J. E. Fischer, J. Lefebvre, M. Radosavljevic, J. Hone, and A. T. Johnson, Phys. Rev. B **61**, 4526 (2000).

[23] J. Zhao, A. Buldum, J. Han, and J. P. Lu, Phys. Rev. Lett. **85**, 1706 (2000).

[24] P. Dubot and P. Cenedese, Phys. Rev. B **63**, 241402(R) (2001).

[25] T. Kar, J. Pattanayak, and S. Scheiner, J. Phys. Chem. A **105**, 10397 (2001).

[26] J. L. Yang, H. J. Liu, and C. T. Chan, Phys. Rev. B **64**, 085420 (2001).

[27] V. Meunier, J. Kephart, C. Roland, and J. Bernholc, Phys. Rev. Lett. **88**, 075506 (2002).

[28] E. C. Lee, Y. S. Kim, Y. G. Jin, and K. J. Chang, Phys. Rev. B **66**, 073415 (2002).

[29] Y. Liu, H. Yukawa, and M. Morinaga, Mol. Cryst. Liq. Cryst. **387**, 99 (2002).

[30] Y. Liu, H. Yukawa, and M. Morinaga, Adv. Quantum Chem. **42**, 315 (2003).

[31] Z. Zhou, X. P. Gao, J. Yan, D. Y. Song, and M. Morinaga, J. Phys. Chem. B **108**, 9023 (2004).

[32] A. Udomvech, T. Kerdcharoen, and T. Osotchan, Chem. Phys. Lett. **406**, 161 (2005).

[33] M. W. Zhao, Y. Y. Xia, X. D. Liu, Z. Y. Tan, B. D. Huang, F. Li, Y. J. Ji, and C. Song, Phys. Lett. A **340**, 434 (2005).

[34] M. W. Zhao, Y. Y. Xia, and L. M. Mei, Phys. Rev. B **71**, 165413 (2005).

[35] Z. Zhou, J. J. Zhao, X. P. Gao, Z. F. Chen, J. Yan, P. V. Schleyer, and M. Morinaga, Chem. Mater. **17**, 992 (2005).

[36] G. Mpourmpakis, E. Tylianakis, D. Papanikolaou, and G. E. Froudakis, J. Nanosci. Nanotechnol. **6**, 3731 (2006).

[37] Z. H. Yang, Y. H. Zhou, S. B. Sang, Y. Feng, and H. Q. Wu, Mater. Chem. Phys. **89**, 295 (2005).

[38] C. Garau, A. Frontera, D. Quinonero, A. Costa, P. Ballester, and P. M. Deya, Chem. Phys. Lett. **374**, 548 (2003).

[39] C. Garau, A. Frontera, D. Quinonero, A. Costa, P. Ballester, and P. M. Deya, Chem. Phys. **303**, 265 (2004).

[40] K. Nishidate and M. Hasegawa, Phys. Rev. B **71**, 245418 (2005).

[41] P. Hohenberg and W. Kohn, Phys. Rev. **136**, B864 (1964).

[42] M. Bockstedte, A. Kley, J. Neugebauer, and M. Scheffler, Comput. Phys. Commun. **107**, 187 (1997).

[43] J. P. Perdew and Y. Wang, Phys. Rev. B **45**, 13244 (1992).

[44] N. Troullier and J. L. Martins, Phys. Rev. B **43**, 1993 (1991).

[45] L. Kleinman and D. M. Bylander, Phys. Rev. Lett. **48**, 1425 (1982).

[46] M. Fuchs and M. Scheffler, Comput. Phys. Commun. **119**, 67 (1999).

[47] M. Khantha, N. A. Cordero, L. M. Molina, J. A. Alonso, and L. A. Girifalco, Phys. Rev. B **70**, 125422 (2004).

[48] X. Gonze, J. M. Beuken, R. Caracas, F. Detraux, M. Fuchs, G. M. Rignanese, L. Sindic, M. Verstraete, G. Zerah, F. Jollet, M. Torrent, A. Roy, M. Mikami, P. Ghosez, J. Y. Raty, and D. C. Allan, Comput. Mater. Sci. **25**, 478 (2002).

[49] W. Yang, J. Chem. Phys. **94**, 1208 (1991).

[50] F. B. C. Machado, R. Bravo, and O. Roberto-Neto, J. Mol. Struct.: THEOCHEM **464**, 7 (1999).

[51] K. Schwarz, P. Blaha, and G. K. H. Madsen, Comput. Phys. Commun. **147**, 71 (2002).

[52] P. Blaha, K. Schwarz, G. K. H. Madsen, D. Kvasnicka, and J. Luitz, *WIEN2k, An Augmented Plane Wave Plus Local Orbitals Program for Calculating Crystal Properties* (Technische Universität Wien, Vienna, 2001).

[53] H. J. Monkhorst and J. D. Pack, Phys. Rev. B **13**, 5188 (1976).

[54] A. D. Becke, Phys. Rev. A **38**, 3098 (1988).

[55] C. Lee, W. Yang, and R. G. Parr, Phys. Rev. B **37**, 785 (1988).

[56] L. A. Girifalco, M. Hodak, and R. S. Lee, Phys. Rev. B **62**, 13104 (2000).

[57] J. A. Alonso and N. A. Cordero, Int. J. Quantum Chem. **56** (Suppl. 29) 49 (1995).

[58] G. Herzberg, *Spectra of Diatomic Molecules* (Van Nostrand Reinhold, New York, 1950).

[59] E. Kaxiras and J. Erlebacher, Phys. Rev. Lett. **72**, 1714 (1994).

[60] J. Merikoski, I. Vattulainen, J. Heinonen, and T. AlaNissila, Surf. Sci. **387**, 167 (1997).

[61] F. Montalenti and R. Ferrando, Phys. Rev. B **59**, 5881 (1999).

[62] H. J. W. Zandvliet, T. M. Galea, E. Zoethout, and B. Poelsema, Phys. Rev. Lett. **84**, 1523 (2000).

[63] P. Boguslawski and J. Bernholc, Phys. Rev. Lett. **88**, 166101 (2002).

[64] A. G. Naumovets, Physica A **357**, 189 (2005).

[65] D. S. Sholl and K. A. Fichthorn, Phys. Rev. Lett. **79**, 3569 (1997).

[66] D. S. Sholl and C. K. Lee, J. Chem. Phys. **112**, 817 (2000).

[67] A. Striolo, Nano Lett. **6**, 633 (2006).

[68] S. Berneche and B. Roux, Nature (London) **414**, 73 (2001).

[69] J. H. Morais-Cabral, Y. F. Zhou, and R. MacKinnon, Nature (London) **414**, 37 (2001).

[70] M. Compoint, P. Carloni, C. Ramseyer, and C. Girardet, Biochim. Biophys. Acta **1661**, 26 (2004).